Available online at www.sciencedirect.com
SCIENCE DIRECT
Journal of Crystal Growth 292 (2006) 149–154
JOURNAL OF CRYSTAL GROWTH
www.elsevier.com/locate/jcrysgro

Growth and characterization of $LiYF_4$:Nd single crystal fibres for optical applications

A.M.E. Santo[a], A.F.H. Librantz[a], L. Gomes[a], P.S. Pizani[b], I.M. Ranieri[a], N.D. Vieira Jr.[a], S.L. Baldochi[a,*]

[a]*Instituto de Pesquisas Energéticas e Nucleares, IPEN-CLA, 05508-900, São Paulo, SP, Brazil*
[b]*Physics Department, Universidade Federal de São Carlos, UFSCar, São Paulo, SP, Brazil*

Received 10 October 2005; received in revised form 29 March 2006; accepted 30 March 2006
Communicated by R.S. Feigelson
Available online 13 June 2006

Abstract

The micro-pulling-down technique has been employed to grow long and regular in diameter Nd-doped $LiYF_4$ single crystal fibres. The effective distribution coefficient of Nd^{3+} ion in the YLF crystal fibres was estimated. The optical absorption and emission of an YLF:Nd bulk crystal and YLF:Nd crystal fibre were compared. The absorption bands of the Nd^{3+} ion, in the visible and in the near infrared, are similar for both materials. The fibre showed an emission band with maximum at 1047 nm and luminescence lifetime of the $^4F_{3/2}$ state of 390 μs while the bulk crystal exhibits the luminescence lifetime of 460 μs.
© 2006 Elsevier B.V. All rights reserved.

PACS: 81.10.Fq; 78.20.−e

Keywords: A2. Micro-pulling-down growth; B1. Fluorides; B1. YLF; B2. Single crystal fibres; B3. Laser-crystals

1. Introduction

The development of compact laser sources in the infrared spectral region has driven the investigations on active laser media based in all-solid-state lasers by direct diode pumping using up conversion of excitation in Nd^{3+}-doped materials [1–3]. The production of laser crystals in the fibre geometry certainly will collaborate with the improvement of highly efficient and compact laser systems with lower costs and greater versatility than conventional ones.

The first single crystal fibres of YAG:Nd for laser applications were grown by the laser heating pedestal growth (LHPG) method in the middle of 1970s [4]. In the end of 1990s, Chani et al. [5] reported the growth of long Nd-doped YAG fibres by the micro-pulling-down (μ-PD) technique.

The $LiYF_4$ (YLF) crystal has been widely employed as host for Nd^{3+} doping, which exhibits laser emission centred at 1.047 μm (π-polarization) and at 1.053 μm (σ-polarization) that are useful for optical applications. This host presents some advantages over YAG crystal, i.e. polarized fluorescence and longest fluorescence lifetime, lower thermal lensing effect and better Q-switched laser performance [6]. Moreover, fluoride crystals doped with Nd^{3+} ions are promising laser media in the ultraviolet spectral region (UV 190–270 nm) [7], that is interesting as a tool for the airborne environmental monitoring by LIDAR (light detection and ranging) [8]. In medicine, it could be useful for the asepsis in chirurgical procedures [9]. Usually, asepsis is done by conventional UV lamp sources, which are big in size and not portable. The use of UV lasers is a possible solution in instrumental asepsis and hygiene, which could solve problems with instrumental connections that are usually difficult to handle with sterility. Also a compact laser device would be well adjusted to the urgency mobile medicine, for which care must be given rapidly and safely.

*Corresponding author. Tel.: +55 11 3816 9303; fax: +55 11 3816 9315.
E-mail address: baldochi@ipen.br (S.L. Baldochi).

0022-0248/$ - see front matter © 2006 Elsevier B.V. All rights reserved.
doi:10.1016/j.jcrysgro.2006.03.054

The purity level of the reagents and spurious contamination arising from the growth atmosphere are the main problems faced in the growth of fluoride crystals. Besides, high structural and optical quality of the Nd-doped YLF crystal is required when pumping it with high power diode lasers. Most enhanced quality has been found in bulk crystals grown by Czochralski (Cz) technique over other growth techniques from the melt. Relatively long fibres of undoped YLF (60 mm) with a constant diameter of 0.8 mm and highly transparent were previously obtained by the μ-PD method [10]. The purpose of the current work is the growth and characterization of Nd-doped YLF single crystal fibre for optical applications with similar properties as the bulk grown by Cz technique.

2. Experimental procedure

2.1. Crystal fibre growth

The phase-diagram of the system LiF–YF_3 suggested by Thoma et al. [11] is shown in Fig. 1. According to the diagram, the YLF melts incongruently and the stoichiometric solid phase at point '*b*' is only obtained from a peritectic reaction. In order to avoid the nucleation of YF_3, the actual composition is slightly enriched in LiF, shown as point 'a'. The compositional interval between points '*a*' and '*b*', depends on the empiric aspects, as growth atmosphere and the reagents grades. The congruent or incongruent melting feature of the YLF compound is extensively discussed in the literature [10–15].

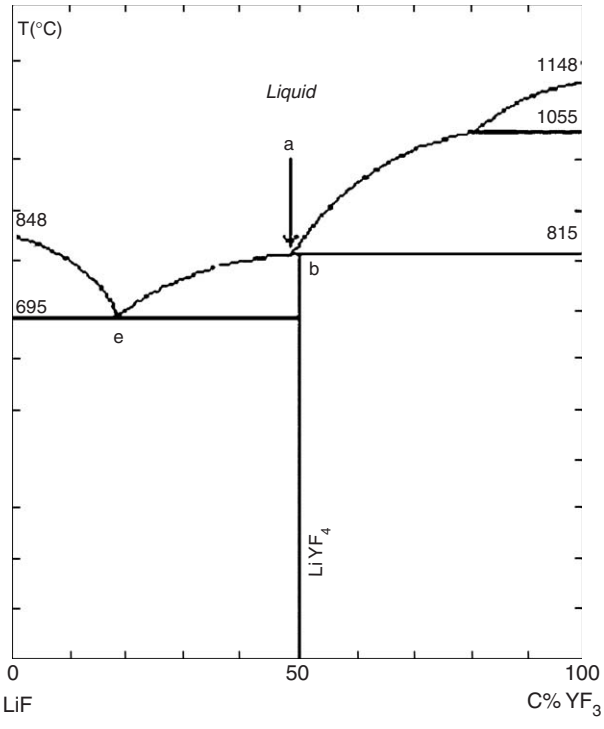

Fig. 1. Phase-diagram of the system LiF–YF_3 suggested by Thoma et al. [11].

The starting material for the fibre growth by the μ-PD method was prepared as described in a previous work for the preparation of undoped YLF fibres [10]. The stoichiometric YLF initial charge was enriched at 5 mol% in LiF, which corresponds to the YF_3:LiF proportion of 49:51 mol% in the melt. The Nd ions were added to the compound as substitution to the Y ion with nominal concentration of 1.7 mol%. The mixture was placed in platinum crucibles, with volume close to 1 cm^3, and melted under a mixed flow of argon (75%) and CF_4 (25%). The fibre was pulled down with a constant rate of 0.75 $mm \cdot min^{-1}$ from a capillary with inner diameter of 0.8 mm and length of about 2.0 mm. A *c*-oriented fibre of undoped YLF was utilized as seed.

2.2. Raman spectroscopy

Depolarized micro-Raman spectroscopy, in the range of 200–500 cm^{-1}, was employed to compare the optical and structural properties of the undoped fibre (used as seed) with those of YLF bulk crystal (grown by Cz technique). Raman scattering was measured along the length of the as-grown single-crystal fibre excited, at room temperature, by the 476.4 nm line of an argon laser. This laser line was chosen since it does not excite any luminescence close to the spectral range of the expected Raman scattered photons. Due to the small fibre diameter, the laser beam was focused by a microscope on the sample surface with an incident diameter of 1 μm. The micro-Raman measurements were performed using a triple monochromator (Jobin–Yvon, model T 64000) spectrometer.

2.3. Chemical analysis

The X-ray fluorescence was accomplished in order to determine the Nd concentration along the fibre. It is pointed out that, using this technique, it is possible to perform a quantitative and non-destructive analysis in the as-grown sample [16]. The measurement was taken longitudinally by energy dispersion radiation from Rh tube (50 kV/100 μA), using a Shimatsu Instruments equipment, model EDX-900. The scanning was done with a pass of 1 cm and count time of 100 s per point.

2.4. Optical characterization

The optical spectroscopy was performed using a spectrophotometer CARY/OLIS 17 interfaced to a micro-computer. The absorption spectra were taken from visible to near infrared range down to 850 nm. The emission spectra were obtained by exciting the samples at 520 nm with a pulsed laser (pulse duration of 4 ns, 10 Hz). The sample point and the gate width were 200 μs and 2 ns, respectively.

3. Results and discussion

3.1. Raman spectroscopy

For a perfect single crystal, the expected Raman spectrum should be composed by delta function peaks at the optical mode frequencies of the fundamental transitions in the reciprocal lattice. The base-width of the first-order peaks results from several factors as instrumental set, anharmonic interactions among phonons, phonons coupling with other excitations, lattice long-range disorder, structural defects and others [17]. The Raman spectra of crystals with the same chemical composition and crystallographic orientation permit to perform a comparative structural analysis. This can be done by the relative broadness evaluation of the main Raman peaks at low frequencies, since the instrumental set keeps unchanged, that is, the base-width given by the instrumental contribution in the spectra is fixed.

Fig. 2 shows the Raman spectrum obtained for both undoped YLF samples: a bulk crystal grown by Cz technique and the fibre grown by the μ-PD technique used as seed for the doped fibre growth. Both single crystals were grown in the *c*-axis orientation.

The fitting curve values and frequencies of the Raman peaks for the YLF bulk and fibre crystals are listed in Table 1. The samples show similar Raman spectra, so their structural qualities are comparable. All peaks are assigned to the $LiYF_4$ structure symmetry [18,19]. Some peaks were not detected comparing with those identified in the literature due to the polarization lack and noise level.

3.2. YLF:Nd grown fibres

Homogeneous Nd-doped YLF single crystal fibres with diameter of 0.6 mm and total length of 50 mm were obtained. The fibres showed a peritectic transient with length of approximately 10 mm, which is opaque and brittle. The length of the stoichiometric phase was 40 mm. Fig. 3 shows the typical as-grown fibre. Micro-cracks and segregation were observed in small regions just at the beginning of the YLF phase formation (Fig. 4a). These effects have been associated to the sudden temperature and compositional changes at the solid/liquid interface during the exothermal peritectic reaction [20]. Thereafter, the stoichiometric phase is bright, transparent and free of cracks in its majority (Fig. 4b).

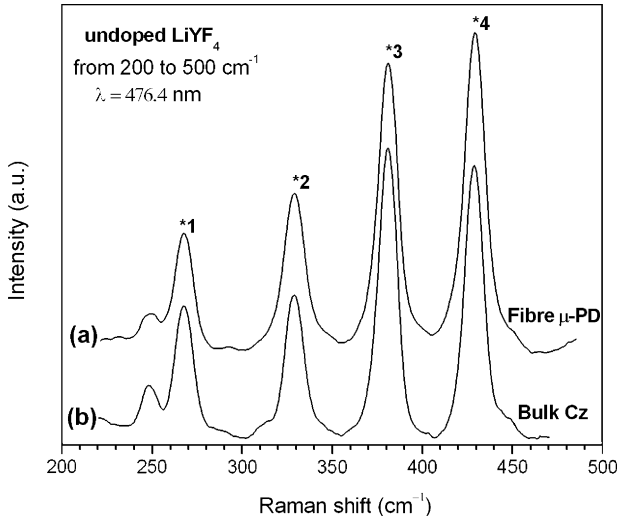

Fig. 2. Raman spectra of undoped YLF crystal at ambient temperature: (a) fibre grown by the μ-P technique, and (b) bulk grown by Czochralski technique.

Table 1
Fitting results of the Raman spectra of the undoped YLF fibre and YLF bulk crystal

Peak number	Raman shift	Bulk crystal Czochralski (cm^{-1})	Crystal fibre μ-PD (cm^{-1})	Phonon simmetry [19]
1	Centred position	267.5	267.7	A_g
	Bandwidth $\frac{1}{2}h$	10.2	10.1	
2	Centred position	328.7	329.1	E_g
	Bandwidth $\frac{1}{2}h$	10.5	10.7	
3	Centred position	381.1	380.9	B_g
	Bandwidth $\frac{1}{2}h$	10.4	10.3	
4	Centred position	428.7	429.2	A_g
	Bandwidth $\frac{1}{2}h$	10.4	10.1	

3.3. Dopant distribution

The relative concentration of the Nd^{3+} ions along the stoichiometric phase is shown in Fig. 5. Here, the origin of the upper *x*-axis corresponds to the first solids of the YLF phase along the fibre. The Nd^{3+} distribution shows a transient at the beginning of the YLF phase, labelled as initial transient (IT). After a given position in the fibre growth axis, approximately 10 mm from the formation of the stoichiometric phase YLF, the Nd^{3+} concentration reaches its maximum, very close to the nominal concentration. After this initial transient, the Nd content is uniform along the fibre, labelled as steady state (SS).

Axially homogeneous fibres can be grown under precise control of the meniscus geometry, which influences considerably the segregation during the μ-PD fibre pulling. The solute initial transient in fibres pulled by the μ-PD method can be described by the classical Pfann's relationship. The liquid zone covers the meniscus height and the capillary channel length [21].

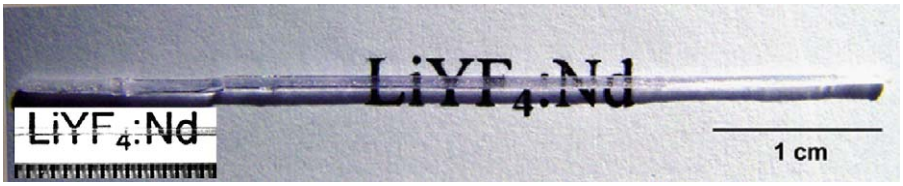

Fig. 3. As-grown Nd-doped YLF fibre with nominal concentration of 1.7 mol% of Nd^{3+} obtained by μ-PD technique.

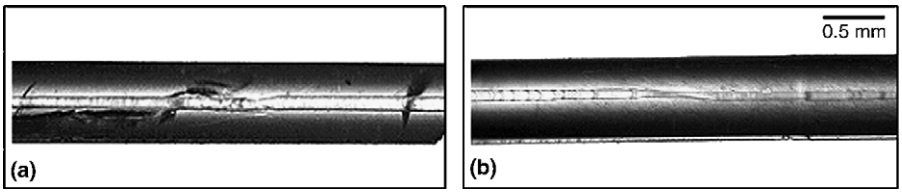

Fig. 4. Optical microscopy of as-grown Nd-doped YLF fibres (scale in mm).

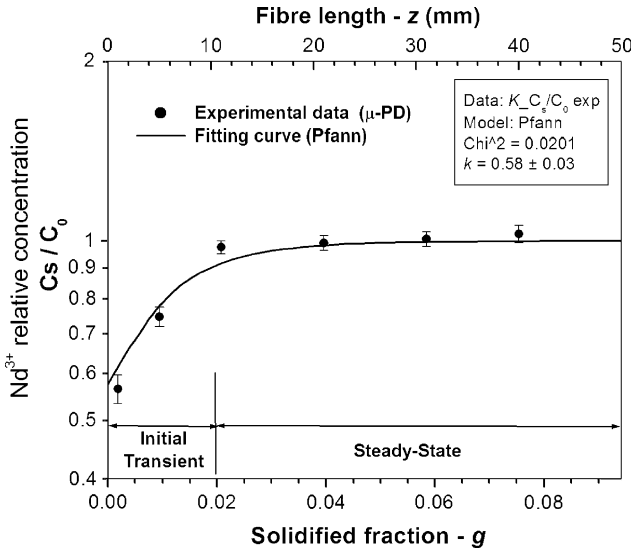

Fig. 5. Relative concentration and distribution fitting curve of the Nd^{3+} ions along the YLF fibre grown by the μ-PD technique with nominal concentration of 1.7 mol% of Nd^{3+}.

The distribution coefficient k was estimated by fitting the experimental results accordingly:

$$\frac{C_s}{C_0} = \left[1 - (1-k)\exp\left(-k\frac{x}{l}\right)\right], \quad (1)$$

where C_s is the Nd^{3+} concentration at a distance x from the beginning of the solidified YLF phase along the fibre; C_0 is the nominal Nd^{3+} concentration and l is the liquid zone length.

Fig. 5 also shows the data fit of the Nd^{3+} relative concentration along the YLF:Nd fibre, considering $C_0 = 1.7$ mol% and $l = 2.5$ mm. There is a good fitting of the experimental data with the theoretical equation. The distribution coefficient k was estimated as 0.58 ± 0.03. This value is greater than those found for Nd^{3+} in YLF bulk crystals grown by the Cz technique, where k is about 0.33 [22]. The Nd^{3+} incorporation and distribution is enhanced in the grown YLF fibres.

In general, the values of k observed in single crystals grown by the μ-PD technique are higher than those grown by Cz technique [23–25]. It is an intrinsic effect of the μ-PD method, influencing the thermodynamic properties in the capillary and meniscus region, improving the melt flow and solute stirring close to the interface solid–liquid [26,27].

3.4. Optical spectroscopy

The optical properties of the YLF fibre doped with a nominal concentration of 1.7 mol% of Nd were compared with those measured for an YLF bulk crystal doped with 1 mol % (Nd) grown by Cz technique.

Fig. 6 shows both absorption spectra of the fibre and the bulk crystals in the visible and near infrared regions. In general, the absorption bands of Nd^{3+} in the YLF fibre exhibited similar multiplets structures compared to the known absorption bands of YLF:Nd crystal, which indicates that the YLF fibre has a single crystal structure from the point of view of absorption transitions of Nd^{3+}.

Fig. 7 shows the emission spectra of the fibre and the bulk crystals around 1054 nm by pulsed laser excitation at 520 nm. The fibre showed an emission band with maximum at 1047 nm raw compatible with $(\pi+\sigma)$ polarization when compared with the pure $(\pi+\sigma)$ emission polarization measured for the bulk crystal perfectly oriented with c-axis perpendicular to the emission collection. Small deviations from the c-axis in the fibre can introduce significant changes in the polarized composition of the 1047 nm emission band related to the one measured for YLF bulk crystal $(\pi+\sigma)$ polarized. An analysis of the misfit towards the c-axis and the pulling direction must be carried-out in further experiments.

The luminescence lifetime of the $^4F_{3/2}$ state of Nd^{3+} was measured for both materials: YLF:Nd bulk and YLF:Nd fibre crystals. This level was attained by pumping direct the

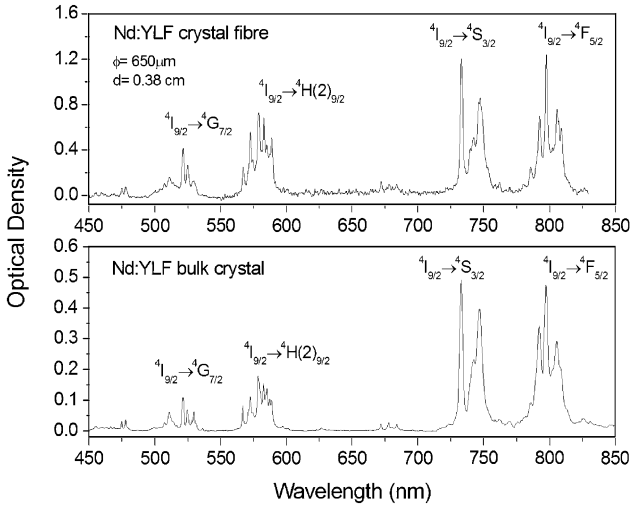

Fig. 6. (a) Absorption spectrum of the YLF:Nd bulk crystal and (b) absorption spectrum of the Nd-doped YLF fibre for the spectral range from 450 to 850 nm.

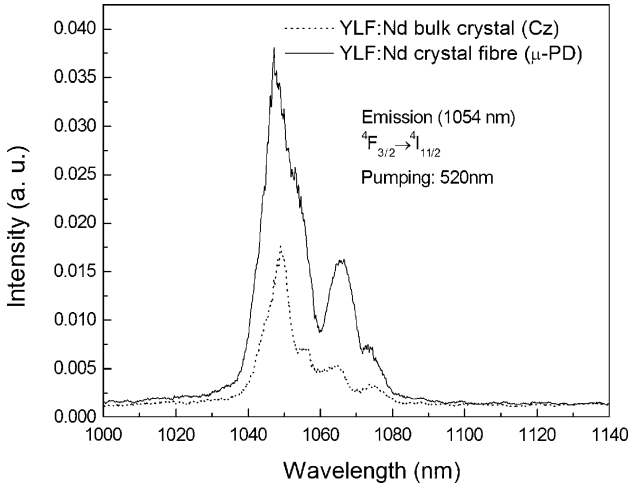

Fig. 7. Emission spectrum of the Nd-doped YLF bulk crystal (doted line) and emission spectrum of the Nd-doped YLF fibre (solid line) around 1054 nm. The sample point and the gate width were 200 ms and 2 ns, respectively.

$^4G_{7/2}$ level which quickly relaxes to the $^4F_{3/2}$ state by pumping it with a pulsed laser at 520 nm with a pulsed duration of 4 ns (10 Hz). The results are shown in Fig. 8.

Fig. 8a shows that the luminescence lifetime of the $^4F_{3/2}$ observed for the Nd-doped YLF fibre is of 390 μs while the Nd-doped YLF crystal (Fig. 8b) exhibits the luminescence lifetime of 460 μs. The decreasing observed in the luminescence lifetime of ~17% for the fibre (doped with 1.7 mol% of Nd) with respect to the bulk crystal (doped with 1 mol% of Nd) is explained by the cross relaxation process between Nd^{3+} ions, which is strongly dependent with its concentration in the host. Increasing the Nd^{3+} concentration increases the cross relaxation process that quenches the $^4F_{3/2}$ luminescence. This leads to a luminescence efficiency decreasing.

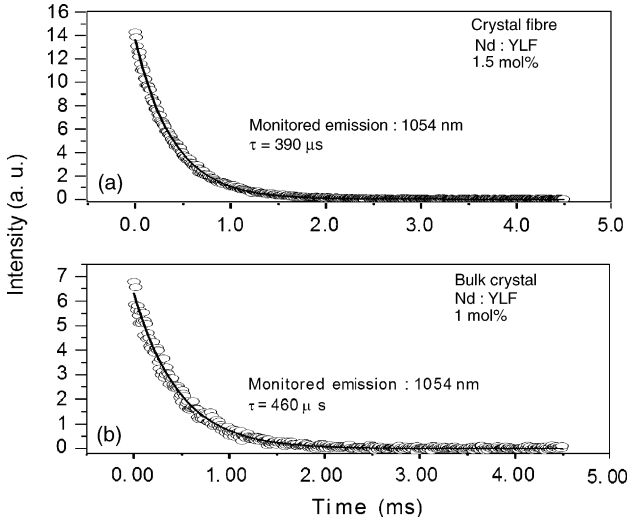

Fig. 8. (a) Luminescence lifetime of $^4F_{3/2}$ level in YLF:Nd^{3+} fibre and (b) luminescence lifetime of the $^4F_{3/2}$ in the YLF:Nd^{3+} bulk crystal (emission at 1054 nm).

4. Conclusion

Regular and transparent Nd-doped YLF single-crystal fibres were successfully grown by the μ-PD technique with uniform diameter of 0.6 mm and length of 50 mm. The Nd^{3+} concentration along the fibre is uniform after a short initial transient. The effective distribution coefficient of 0.58 indicates that the Nd adding in the YLF host is enhanced in the fibre compared to bulk crystals grown by Cz technique. Therefore, the Nd^{3+} concentration in this host for laser applications is limited due to the cross-relaxation effects, as observed in the optical emission and fluorescence lifetime results. However, the similarity observed within absorption bands around 800 nm, comparing the fibre (grown by the μ-PD technique) and the bulk crystal (grown by Cz technique), makes us to consider the YLF:Nd fibre as an important material to construct a compact all-solid-state lasers based on high power diode laser pumping.

Acknowledgements

The authors are grateful to FAPESP for the financial support under projects 00/00234-1 and 01/7337-3, and to V.L.R. Salvador (CQMA/IPEN) for the X-ray fluorescence analysis.

References

[1] J. Stone, C.A. Burrus, A.G. Dental, B.I. Miller, Appl. Phys. Lett. 29 (1976) 37.
[2] M. Fejer, J. Nightingale, G. Magel, R. Byer, Lase Focus/Electro Optics, October 1985, p. 60
[3] R. Balda, J. Fernandez, M. Sanz, A. De Pablos, J.M. Fdez-Navarro, J. Mugnier, Phys. Rev. B 61 (2000) 3384.
[4] C.A. Burrus, J. Stone, J. Appl. Phys. Lett. 26 (1975) 318.

[5] V.I. Chani, A. Yoshikawa, Y. Kuwano, K. Hasegawa, T. Fukuda, J. Crystal Growth 204 (1999) 155.
[6] T.M. Pollack, W.F. Wing, R.I. Grasso, E.P. Chicklis, H.P. Jenssen, IEE J. Quantum Electron. QE- QE-18 (1982) 159.
[7] A.F.H. Librantz, L. Gomes, L.V.G. Tarelho, I.M. Ranieri, J. Appl. Phys. 95 (2004) 4.
[8] R. Mussa, S. Argiró, R. Cester, M. Chiosso, A. Filipi, M. Horvat, J. Matthews, M. Mostafá, M. Roberts, G. Sequeiros, et al., Nucl. Instrum. Methods A 183 (2004) 1.
[9] K. Kleinermanns, J. Wolfrum, Angew. Chem. 26 (1) (2003) 38.
[10] A.M.E. Santo, I.M. Ranieri, G.E.S. Brito, B.M. Epelbaum, S.P. Morato, N.D. Vieira Jr., S.L. Baldochi, J. Crystal Growth 275-3 (2005) 528.
[11] R.E. Thoma, C.F. Weaver, H.A. Friedman, H. Insley, H.A. Harris, H.A. Yakel Jr., J. Phys. Chem. 65 (1961) 1096.
[12] R.C. Pastor, M. Robinson, W.M. Akutawaga, Mater. Res. Bull. 10 (1975) 501.
[13] H. Safi, I.R. Harris, B. Cockayne, J.G. Plant, J. Mater. Sci. 16 (1981) 3203.
[14] R. Uhrin, R.F. Belt, J. Crystal Growth 38 (1977) 38.
[15] B.P. Sobolev, Crystallogr. Rep. 47 (2002) S63.
[16] E.P. Bertin, Quantitative analysis, in: Principles and Practice of X-ray Spectrometric Analysis, second ed, Plenum Press, New York, 1975 (Chapter 14).
[17] P.W. Atkins, Spectroscopy 1: rotational and vibrational spectra, in: Physical Chemistry, 5th ed, Oxford University Press, Oxford, UK, 1994, pp. 539–586 (Chapter 16).
[18] E. Sarantopoulou, Y.S. Raptis, E. Zouboulis, C. Raptis, Phys. Rev. B 59 (1999) 4154.
[19] E. Schullteiss, A. Scarman, D. Schwabe, Phys. Status Solidi B 138 (1986) 465.
[20] W.D. Callister Jr., Phase diagrams, in: Materials Science and Engineering—An Introduction, sixth ed, Wiley, New York, 2003 (Chapter 9.12).
[21] B.M. Epelbaum, Practice of micro pulling down growth, in: T. Fukuda, P. Rudolph, S. Uda (Eds.), Fibre Crystal Growth from the Melt, Advances in Materials Reserch, vol. 6, Springer, Berlin, 2004.
[22] I.M. Ranieri, N.M. Moraes, H.M. Shihomatsu, S.P. Morato, XII National Meeting on Condensed Matter Physics, XII ENFMC, São Lourenço, MG, Brazil, 1999, p. 247.
[23] V.I. Chani, A. Yoshikawa, Y. Kuwano, K. Hasegawa, T. Fukuda, J. Crystal Growth 204 (1–2) (1999) 155.
[24] V.I. Chani, A. Yoshikawa, Y. Kuwano, K. Inaba, K. Omote, T. Fukuda, Mater. Res. Bull. 35 (10) (2000) 1615.
[25] B. Hautefeuille, K. Lebbou, C. Dujardin, J.M. Fourmigue, L. Grosvalet, O. Tillement, C. Pédrini, J. Crystal Growth 289 (2006) 172.
[26] N. Schäfer, T. Yamada, K. Shimamura, H.J. Koh, T. Fukuda, J. Crystal Growth 166 (1996) 675.
[27] H.J. Koh, N. Schäfer, K. Shimamura, T. Fukuda, J. Crystal Growth 167 (1996) 38.